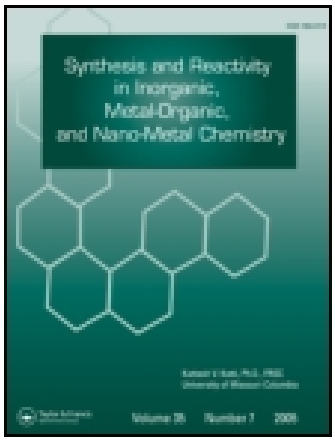

Synthesis and Reactivity in Inorganic, Metal-Organic, and Nano-Metal Chemistry

Publication details, including instructions for authors and subscription information: http://www.tandfonline.com/loi/lsrt20

Oxovanadium(IV) Schiff Base Complex Derived From Phenylalanine Analogue Containing 2,3-Diaminopropionic Acid (DAP): Synthesis, Computational Study, and Biological Evaluation

Le Wei[ab], Xia Yang[a], Zeng-Qiang Gao[c], Dong-Qi Wang[a], Jing-Quan Xue[ad], Wen-Jiang Yang[ad], Jian-Jun Wang[ad], Yan-Hua Zhang[ad], Guo-Liang Fang[b] & Yu Liu[ad]

[a] Key Laboratory of Nuclear Radiation and Nuclear Energy Technology, Beijing, P. R. China

[b] University of Chinese Academy of Sciences, Beijing, P. R. China

[c] Beijing Synchrotron Radiation Facility, Institute of High Energy Physics, Chinese Academy of Sciences, Beijing, P. R. China

[d] Beijing Engineering Research Center of Radiographic Techniques and Equipment, Beijing, P. R. China

Accepted author version posted online: 16 Sep 2014.Published online: 15 Oct 2014.

To cite this article: Le Wei, Xia Yang, Zeng-Qiang Gao, Dong-Qi Wang, Jing-Quan Xue, Wen-Jiang Yang, Jian-Jun Wang, Yan-Hua Zhang, Guo-Liang Fang & Yu Liu (2015) Oxovanadium(IV) Schiff Base Complex Derived From Phenylalanine Analogue Containing 2,3-Diaminopropionic Acid (DAP): Synthesis, Computational Study, and Biological Evaluation, Synthesis and Reactivity in Inorganic, Metal-Organic, and Nano-Metal Chemistry, 45:3, 455-467, DOI: 10.1080/15533174.2013.841205

To link to this article: http://dx.doi.org/10.1080/15533174.2013.841205

Synthesis and Reactivity in Inorganic, Metal-Organic, and Nano-Metal Chemistry (2015) 45, 455–467

ISSN: 1553-3174 print / 1553-3182 online
DOI: 10.1080/15533174.2013.841205

Oxovanadium(IV) Schiff Base Complex Derived From Phenylalanine Analogue Containing 2,3-Diaminopropionic Acid (DAP): Synthesis, Computational Study, and Biological Evaluation

LE WEI[1,2], XIA YANG[1], ZENG-QIANG GAO[3], DONG-QI WANG[1], JING-QUAN XUE[1,4], WEN-JIANG YANG[1,4], JIAN-JUN WANG[1,4], YAN-HUA ZHANG[1,4], GUO-LIANG FANG[2], and YU LIU[1,4]

[1]*Key Laboratory of Nuclear Radiation and Nuclear Energy Technology, Beijing, P. R. China*
[2]*University of Chinese Academy of Sciences, Beijing, P. R. China*
[3]*Beijing Synchrotron Radiation Facility, Institute of High Energy Physics, Chinese Academy of Sciences, Beijing, P. R. China*
[4]*Beijing Engineering Research Center of Radiographic Techniques and Equipment, Beijing, P. R. China*

Received 6 June 2013; accepted 1 September 2013

Reduced Schiff base ligand by condensation of phenylalanine analogue containing 2,3-diaminopropionic acid (DAP) with salicylaldehyde and its oxovanadium(IV) complex have been prepared. Chemical and structural properties were fully characterized. Density functional theory was used to pin down the structure combined with IR. The natural bond orbital analysis and energy calculations indicate that tetracoordinated complex of R-type is the most probable structure where vanadium atom is coordinated to $2 \times O_{phenolate}$ and $2 \times N_{imine}$ of the ligand. By biological evaluation, the metal complex exhibits antibacterial activity against four bacterial strains and antitumor activity against two tumor cell lines.

Keywords: reduced Schiff base, oxovanadium(IV) complex, density functional theory (DFT), biological evaluation

Introduction

Schiff bases are a class of important multidentate structures which are considered to be privileged ligands and exhibit great versatility of coordination patterns to various metals.[1] Transition metal Schiff base complexes are well known as efficient catalysts in both homogeneous and heterogeneous reactions, such as polymerization of olefins,[2] asymmetric chemical transformations,[3] epoxide ring opening,[4] and Diels–Alder reactions.[5] In addition, many Schiff base complexes exhibit biological activities including antibacterial and antitumor activities, and have been studied to understand their biochemical significance and structure–activity relationships.[6] The complexation of biologically active Schiff base ligands with transition metal ions can potentially produce a large number of drug candidates in therapeutical and biomedical fields. Vanadium is an essential element in biological systems. Besides the use of vanadyl Schiff bases as catalysts with good enantioselectivity,[7,8] they also have important applications in the biological field, such as DNA cleavage agent,[9] insulin mimic for the treatment of diabetes,[10] and antitumor agent.[11]

Amino acids are environmentally benign and especially appropriate for synthesis of Schiff base catalysts through condensation of salicylaldehyde and aldehyde derivatives.[12] 2,3-Diaminopropionic acid (DAP), which was discovered in Bombyx[13] and Murchison meteorite,[14] exists widely in nature. Since this kind of amino acid derivatives possess important biological structure, much more attention has been paid by both chemists and biologists for many years.[15–17]

Nevertheless, very limited researches on metal Schiff base complexes derived from DAP or its derivatives are carried out.[18–20] Costa Pessoa et al.[21] explored the chemical properties of vanadyl Schiff base complexes by condensation of DAP with salicylaldehyde using potentiometric and spectroscopic techniques; however, so far theoretical computations have not yet been reported. As is known to all, density functional theory (DFT) computations are quite successful in the description and explanation of transition-metal complexes for their formation, structures, energies, and barriers.[22]

Herein, we synthesize a novel oxovanadium(IV) Schiff base complex (abbr. $V^{IV}O$ complex) derived from phenylalanine

Address correspondence to Yu Liu, Key Laboratory of Nuclear Radiation and Nuclear Energy Technology, Beijing Engineering Research Center of Radiographic Techniques and Equipment, Institute of High Energy Physics, Chinese Academy of Sciences, Beijing 100049, P. R. China. E-mail: yuliu@ihep.ac.cn.
Color versions of one or more of the figures in the article can be found online at www.tandfonline.com/lsrt.

analogue containing DAP, and study the possible coordination structure by DFT computations as well as the biological activities. The antibacterial and antitumor activities are evaluated for potential applications in discovery of new pharmaceuticals in medical field.

Experimental

Materials and Methods

All chemicals and solvents were of reagent grade and used as received from commercial sources without further purification. Ethyl-N-acetyl-3-nitriloalaninate **2** was produced according to the literature.[23]

NMR spectra were recorded on Bruker 400 MHz spectrometer. Chemical shifts were referenced to DMSO-d_6 or D_2O as solvent and TMS as internal standard. ^1H and ^{13}C NMR spectra were obtained and reduced Schiff base ligand **9** was fully assigned with the aids of 2-D NMR Spectroscopy (^1H-^1H COSY, HSQC, and HMBC). Fourier transform infrared (FT-IR) spectroscopy was taken on a Bruker Tensor 27 instrument with KBr disks. Electrospray ionization mass spectra were obtained by using Bruker ESI-Q-TOF-Mass spectrometry. The spectra were measured fully in the positive ion mode and showed the expected molecular ion peaks in all cases. Elemental analysis (C, H, and N) were performed using a Flash EA 1112 model analyzer, and consistent with the composition proposed for the $V^{IV}O$ complex. Melting points (m.p.) were determined on Electrothermal X-4 apparatus.

Synthesis

Products were prepared using modified methods described previously,[15,17,20,21] as shown in Scheme 1.

Ethyl 2-acetamido-2-cyano-3-phenylpropanoate (4)

To a flask containing absolute ethanol (50 mL) was added sodium (0.1495 g, 6.5 mmol) with stirring under Ar. After complete dissolution, **2** (1.0539 g, 6.2 mmol) was added and the solution was stirred at 60°C for 30 min. After cooling down to room temperature, benzyl bromide **3** (1.0589 g, 6.2 mmol) was added. The reaction solution was refluxed overnight and the solvent was removed under vacuum. The resulting residue was treated with H_2O (100 mL) and extracted with EtOAc (3 × 50 mL). The combined organic phase was washed with brine (2 × 50 mL) and dried over $MgSO_4$. The filtrate was concentrated and the obtained solid was crystallized from EtOAc/Hexane (v/v, 1:3) to give white crystals. Yield: 1.5089 g (94%) and m.p. 128.6–130.0°C.

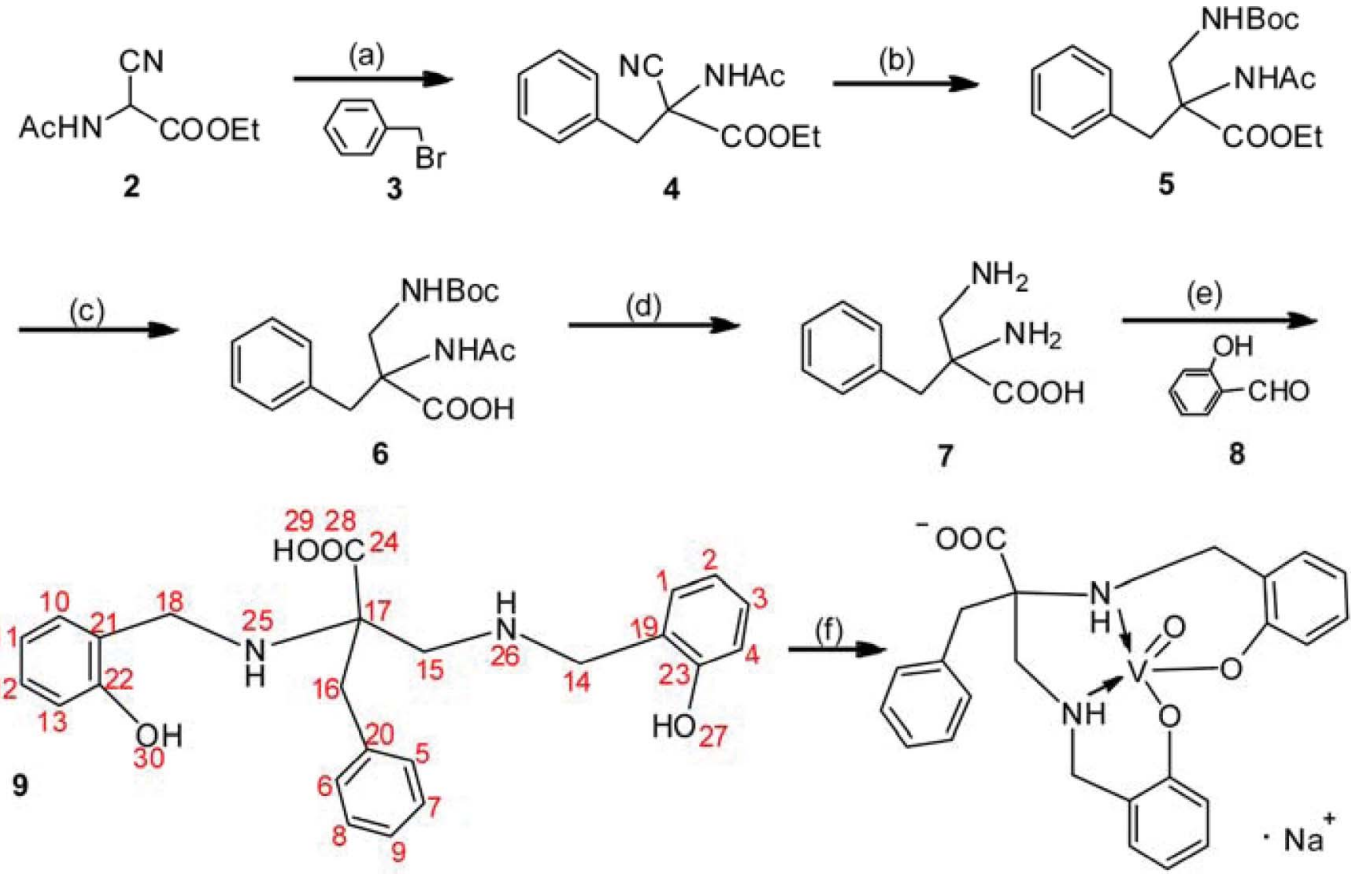

Sch. 1. The reaction conditions are: (a) EtOH, NaOEt, benzyl bromide **3**; reflux (b) (1) MeOH, $NaBH_4$, $NiCl_2$, Boc_2O, (2) diethylenetriamine; (c) (1) NaOH, (2) $NaHSO_4$; (d) (1) HCl, (2) Et_2O, (3) $NaHCO_3$; (e) (1) MeOH, Et_3N, salicylaldehyde **8** (2) MeOH, $NaBH_4$, 0°C; (f) EtOH, NaOH, $VOSO_4$, NaOAc.

ESI-MS: *m/z* 283.1022 [M+Na]. IR (KBr, cm^{-1}): 3,310 (m), 3,067 (w), 3,050 (w), 2,989 (w), 2,933 (w), 1,749 (vs), 1,666 (s), 1,514 (s), 1,501 (sh), 1,456 (m), 1,443 (sh), 1,373 (m), 1,324 (w), 1,303 (w), 1,280 (s), 1,088 (s), 1,043 (s). ^{1}H NMR (400 MHz, DMSO-d_6) δ_H 9.27 (1H, s, N*H*), 7.40–7.21 (5H, m, —C_6H_5), 4.10–3.93 (2H, q, $J = 7.1$ Hz, —CH_2CH_3), 3.37 (1H, d, $J = 13.4$ Hz, —C*H*H—C_6H_5), 3.17 (1H, d, $J = 13.4$ Hz, —CH*H*-C_6H_5), 1.95 (3H, s, —COCH_3), 1.01 (3H, t, $J = 7.1$ Hz, -CH_2CH_3) ppm. ^{13}C NMR (101 MHz, DMSO-d_6) δ_C 169.96, 165.86, 132.24, 130.15, 128.27, 127.93, 117.05, 62.20, 58.62, 40.96, 21.63, 13.54 ppm.

*Ethyl 2-acetamido-2-benzyl-3-[(tert-butoxycarbonyl)amino] propanoate (**5**)*

To the solution of **4** (0.5209 g, 2.0 mmol) in anhydrous MeOH (50 mL) cooled to 0°C were added Boc_2O (0.4583 g, 2.1 mmol) and $NiCl_2{\cdot}6H_2O$ (0.0476 g, 0.2 mmol) to give a pale green solution. $NaBH_4$ (0.6063 g, 16.0 mmol) was added in portions with stirring. The purple mixture was stirred overnight and then diethylenetriamine (0.2 mL) was added. After 1 h, the volatile part of the mixture was removed under vacuum. The residue was partitioned between EtOAc (3×50 mL) and saturated $NaHCO_3$ solution (50 mL). The organic phase was washed with brine (50 mL) and dried over $MgSO_4$. The filtrate was evaporated and the residue was recrystallized from EtOAc/Hexane (v/v, 1:4) to give white crystals. Yield: 0.5597 g (77%) and m.p. 74.0–74.5°C. ESI-MS: *m/z* 387.1896 [M + Na]. IR (KBr, cm^{-1}): 3,400 (s), 3,305 (m), 1,741 (vs), 1714 (vs), 1,650 (s), 1,530 (vs), 1,391 (w), 1,375 (sh), 1,368 (s), 1,339 (w), 1,322 (w), 1,280 (w), 1,252 (s), 1,167 (s), 1,109 (m). ^{1}H NMR (400 MHz, DMSO-d_6) δ_H 7.69 (1H, s, —N*H*COCH$_3$), 7.32–7.11 (5H, m, —C_6H_5), 6.79 (1H, s, —N*H*Boc), 4.02–3.86 (2H, q, $J = 7.1$ Hz, —CH_2CH3), 3.38 (1H, dd, $J = 13.8$ Hz, 6.1 Hz, -CH*H*-), 3.27 (1H, dd, $J = 13.9$ Hz, 6.7 Hz, —C*H*H-), 3.22–3.13 (1H, m, —CH*H*—), 3.01 (1H, d, $J = 13.4$ Hz, —C*H*H—), 1.81 (3H, s, —COCH_3), 1.39 (9H, s, —COOC(CH_3)$_3$), 1.10 (3H, t, $J = 7.1$ Hz, —CH_2CH_3) ppm. ^{13}C NMR (101 MHz, DMSO-d_6) δ_C 170.83, 169.12, 155.69, 135.86, 130.30, 127.83, 126.49, 77.91, 62.43, 60.30, 42.26, 36.96, 28.11, 22.71, 13.77 ppm.

*2-Acetamido-2-benzyl-3-[(tert-butoxycarbonyl)amino] propionic acid (**6**)*

To the aqueous solution of NaOH (30 mL, 0.5 M) was added **5** (1.8222 g, 5.0 mmol). The mixture was stirred at 65°C for 3 h. After complete dissolution of solids, $NaHSO_4$ was added to adjust the pH value to 2–3 and white solid **6** precipitated. After filtration, the solid was washed with water (50 mL) and diethyl ether (50 mL). Yield: 1.3900 g (83%) and m.p. 210.0–211.5°C. ESI-MS: *m/z* 359.1598 [M + Na]. IR (KBr, cm^{-1}): 3,415 (m), 3,255 (m), 3,061 (m), 1,743 (s), 1,688 (vs), 1,667 (vs), 1,559 (m), 1,512 (s), 1,337 (w), 1,317 (w), 1,293 (s), 1,255 (m), 1,110–1,032 (mw), 931 (w).

*2-Benzyl-2,3-diaminopropionic acid (BDAP) (**7**)*

To the aqueous hydrochloric acid solution (4 M, 10 mL) was added **6** (0.8409 g, 2.5 mmol) and the mixture was refluxed overnight. After cooling down to room temperature, the mixture was neutralized by $NaHCO_3$ and washed with diethyl ether. The residual solution was concentrated under vacuum and afforded corresponding product, which could not be separated from NaCl. ^{1}H NMR (400 MHz, D_2O) δ_H 7.30–7.12 (5H, m, Ar-*H*), 3.16 (1H, d, $J = 13.3$ Hz), 3.06 (1H, d, $J = 13.5$ Hz), 2.89 (1H, d, $J = 13.3$ Hz), 2.74 (1H, d, $J = 13.5$ Hz) ppm. ^{13}C NMR (101 MHz, D_2O) δ_C 170.71, 131.52, 130.16, 129.36, 128.66, 61.25, 42.65, 39.37 ppm.

*2-Benzyl-2,3-bis[(2-hydroxybenzyl)amino]propanoic acid (**9**)*

Triethylamine (0.5 mL) was added to a suspension of **7** (6.0 mmol) in anhydrous methanol (20 mL). Small portions of salicylaldehyde (1.7549 g, 14.4 mmol) in MeOH (10 mL) were slowly added to this solution. The color changed to yellow and became darker with the addition. $MgSO_4$ was added and the solution was stirred overnight. After filtration, the filtrate was cooled in ice and the following addition of $NaBH_4$ (1.3255 g, 35.0 mmol) in portions produced white precipitates. Acetic acid was used to adjusted pH to weak acidic. Then the solution was filtered and the obtained white solid was washed with water (2 × 50 mL) and MeOH (2 × 50 mL) and dried under vacuum. Yield: 0.9749 g (40%) and m.p. 229.2–230.4°C. For $C_{24}H_{26}N_2O_4$: Anal. Calcd. C, 70.92; H, 6.45; N, 6.89; Found C, 71.06; H, 6.60; N, 7.04 %. ESI-MS: *m/z* 407.1944 [M + H]. IR (KBr, cm^{-1}): 3,401 (br), 3,219 (w), 3,057 (w), 3,031 (w), 1,613 (vs), 1,595 (vs), 1,548 (sh), 1,490 (s), 1,462 (vs), 1,443 (w), 1,389 (m), 843 (w), 761 (s), 745 (sh). ^{1}H NMR (400 MHz, DMSO-d_6) δ_H 8.17 (4H, br s, Ar—O*H* and N*H*), 7.27–6.66 (13H, m, Ar—*H*), 3.91 (2H, s, —CH_2NHCH_2—), 3.74 (1H, d, $J = 12.6$ Hz, —CNHC*H*H—), 3.61 (1H, d, $J = 12.6$ Hz, —CNHCH*H*—), 2.98 (2H, q, $J = 13.5$ Hz, C_6H_5—CH_2—C—), 2.86 (2H, s, $J = 13.0$ Hz, —CCH_2NH—) ppm. ^{13}C NMR (101 MHz, DMSO-d_6) δ_C 174.08, 156.30, 156.27, 136.52, 130.45, 130.21, 129.52, 129.30, 128.28, 127.87, 126.30, 124.78, 121.39, 118.71, 118.44, 115.38, 115.28, 63.90, 49.95, 47.84, 43.48, 40.05 ppm.

Sodium 2-benzyl-2,3-bis[(2-hydroxybenzyl)amino oxovanadium(IV)] propionate, the $V^{IV}O$ complex

Under Ar atmosphere, reduced Schiff base **9** (0.2029 g, 0.5 mmol) was dissolved in 10 mL ethanol/water (v/v, 1:3) with the aid of a few drops of NaOH aqueous solution (4 M). Then an aqueous solution of sodium acetate (2.5 M, 1 mL) was added. With the addition of $VOSO_4{\cdot}5H_2O$ (0.5 M, 1 mL), the solution gradually turned brown and a grey solid precipitated. After filtered, the precipitate was washed with cold water (5 mL, *ca.* 4°C), ethanol (5 mL) and diethylether (10 mL) in order. After drying under vacuum, product was obtained as grey solid. Yield: 0.1084 g (44%) and m.p. > 300°C. For $C_{24}H_{23}N_2O_5NaV$: Anal. Calcd. C, 58.42; H, 4.70; N, 5.68; Found C, 58.80; H, 4.97; N, 5.92 %. ESI-MS: *m/z* 493.0865 [M]. IR (KBr, cm^{-1}): 3,421 (br), 3,274 (m), 3,126 (mw), 2,928 (m), 2,865 (w), 1,639 (vs), 1,596 (vs), 1,391 (m), 1,338 (w), 1,308 (w), 1,142 (s), 1,080 (m), 1,037 (m), 962 (s), 760 (s), 468 (w), 440 (m). ^{1}H NMR (400 MHz, DMSO-

d_6) δ_H 7.25 (13H, d, $J = 118.3$ Hz), 3.60 (7H, br s), 1.67 (3H, br s) ppm.

Crystallographic Study

Single crystals were obtained by slow evaporation of n-hexane–$CHCl_3$ (**4**) and n-hexane–EtOAc (**6**) solutions at room temperature. Crystallographic data were collected at Beijing Synchrotron Radiation Facility (BSRF) beamline 1W2B, which mounted with a MARCCD-165 detector with storage ring working at 1.89 GeV. In the process, the crystals were protected by liquid nitrogen at 100 K. Data were collected by the program marccd and processed using HKL 2000.[24] The structures were solved by direct methods and refined by full-matrix least-squares on F^2 using SHELXL97 program package.[25] Molecular graphics were provided with ORTEP3.[26] Significant crystal data and structure refinements can be found in Table S1.

Computational Methods

Gaussian09 package[27] was used to perform calculations, based on the basic laws of quantum mechanics, in order to identify the possible structure of ligand **9** and $V^{IV}O$ complex. Gaussian 09 contains a series of electronic structure programs to predict the energies, molecular structures, vibration frequencies, and molecular properties and reactions of molecules in chemical environments.

As shown in Table 1, computations were carried out using DFT[28] at the B3LYP level,[29,30] a hybrid functional combining Becke's 1988 nonlocal exchange[31] with Hartree-Fock exchange along with the Lee-Yang-Parr[32] correlation functional. All possible configurations were fully optimized with a description of V atom by a pseudopotential ECP10MDF[33,34] and all the other elements by 6-31G* basis set.[35] The spin state was set to be doublet for complexes and singlet for ligands.

The nature of the optimized structure was checked using normal-mode frequency analysis (i.e., the real minimum structure must have no negative frequencies). The vibrational frequencies were determined by evaluating analytically the second derivatives of the energy with respect to the nuclear coordinates at the same levels. The B3LYP/6-31G* vibrational frequencies were scaled by a factor of 0.9804.[36]

Antibacterial Assays

The bacteria were cultured in sterile liquid Luria-Bertani (LB) medium (pH 7.2), which was made up of NaCl (1 g), tryptone (1 g), and yeast extract (0.5 g) in 100 mL distilled water at 37°C. The following common infectious agents were used including *Staphylococcus aureus*, *Lactobacillus acidophilus*, *Enterococcus faecalis*, and *Escherichia coli*, which were cultured in 5 mL LB medium at 37°C, 200 rpm for 16 h, and subsequently were applied to biological study.

In the inhibition zone test, the antibacterial activities were evaluated by measuring the diameter of inhibition zone according to the disc-agar diffusion method.[37] The tested compounds were dissolved in DMSO (conc. 1 mg mL^{-1}) and soaked in sterile discs (diam. 5 mm) that were later placed on the seeded plates. After incubation at 37°C for 24 h, the diameter of inhibition zone surrounding each disk was measured. The data presented in Table 2 are the average value from quadruplicate measurements.

Above cultured microbes were also used to study the inhibitory effect on the bacterial growth according to reported methods.[38,39] 16 h later, the synthesized compounds (dissolved in DMSO) were added with increasing concentrations ranging from 0 to 1500 μg mL^{-1} to 1 mL LB containing 0.1 mL inoculum. After incubation for 4 h at 37°C and 200 rpm, the absorbance was measured at 600 nm (OD600) with a microplate reader (SpectraMax M2, Molecular Devices Corp., USA).

Cytotoxicity Assays

Cytotoxicity assays were tested on human lung carcinoma epithelial cell (*A549*) and human cervical carcinoma cell (*Hela*) respectively. The cell viability was evaluated by using a standard Cell Counting Kit-8 (CCK-8) colorimetric assay, performed as follows: Cells were seeded into 96-well sterile plates in 0.1 mL of supplemented Dulbecco's Modified Eagle's Medium (DMEM) at a density of 5×10^3 cells per well and incubated for 24 h at 37°C under 5% CO_2 atmosphere at constant humidity.

Table 1. Mayer bond order analysis of four complexes and relative electronic energies[a] of complexes, Gibbs free energies[b] of complexing reactions, and deformation energies[c] of ligands for four complexes at B3LYP/6-31G* level with ZPE correction.

	Bond	R_$V^{IV}O$ Complex_a	R_$V^{IV}O$ Complex_b	S_$V^{IV}O$ Complex_c	S_$V^{IV}O$ Complex_d
Mayer bond order	V(32)−O(27)	0.86	—	0.85	0.06
	V(32)−O(30)	0.83	0.86	0.82	0.86
	V(32)−N(25)	0.52	0.53	0.06	0.26
	V(32)−N(26)	0.46	—	0.57	0.60
	V(32)−O(28)	—	0.79	—	0.71
	V(32)−O(29)	—	0.06	—	0.05
Energies	$\Delta E_{relative}$	0.00	45.81	26.79	13.74
	$\Delta G_{reaction}$	–814.87	–765.99	–783.31	–802.26
	$\Delta E_{deformation}$	58.97	54.95	70.15	74.29

[a,b,c]Calculated in kcal mol^{-1}. [b]The Gibbs free energy is defined as $\Delta G_{reaction} = G_{complex} - (G_{ligand3-} + G_{VO2+})$.

Table 2. Inhibition zone (mm) of Schiff base ligand **9** and its $V^{IV}O$ complex.

	Diameter			
Sample	*S. aureus* Mean ± RSD	*L. acidophilus* Mean ± RSD	*E. faecalis* Mean ± RSD	*E. coli* Mean ± RSD
Schiff base ligand	0	0	0	0
$V^{IV}O$ complex	8.52 ± 0.388	9.70 ± 0.381	16.51 ± 0.127	9.51 ± 0.338
Standard: Kanamycin	13.58 ± 0.378	16.32 ± 0.309	21.40 ± 0.168	13.17 ± 0.270

After washing each well with phosphate buffered saline (PBS, 0.01 M, pH = 7.4), compounds dissolved in DMEM were added with increasing concentrations ranging from 0 to 1200 μg mL^{-1} to a volume of 0.1 mL per well. Subsequent incubation for another 24 h, culture medium solution of CCK-8 was added to each well and the plate was incubated further for 1 h at 37°C in cell culture incubator in a humidified 5% CO_2 atmosphere. The cell viability was determined by acquiring the absorbance, which was the average value from triplicate measurements at 450 nm (OD450) with the microplate spectrophotometer.

Results and Discussion

Synthesis and Crystal Structure

Scheme 1 provided a general procedure for the synthesis of $V^{IV}O$ complex from reduced Schiff base ligand **9** with DAP aryl-substituted at its α-carbon position. Compound **2** was deprotonated by NaOEt and alkylated by benzyl bromide **3** to give compound **4** in high yield with 94%. The nitrile group was reduced by $NaBH_4$ and then protected by Boc_2O with the catalyst $NiCl_2$ to give compound **5**. This is a novel but key step for designing the protected DAP derivatives in our study.[15] *In situ* hydrolysis of the ethyl ester group resulted in compound **6**. Subsequent deprotection afforded BDAP **7** in D- and L-type forms. This routine synthesis of the phenylalanine analogue avoids using rather expensive reagents/catalyst[16] and exhibits a straightforward and convenient method for BDAP. The formation of Schiff base is usually favored by the presence of dehydrating agents,[40] and therefore $MgSO_4$ was added to remove the water produced in condensation reaction. In order to avoid the imine hydrolysis, the product was further reduced by $NaBH_4$ in methanol after the Schiff base was synthesized. Subsequent reaction of ligand **9** and vanadyl gave the corresponding product $V^{IV}O$ complex.

ORTEP presentations of the molecular structures for compounds **4** and **6** are given in Figure S1. Both **4** and **6** were crystallized in racemic forms in the space groups $P2_1/n$ and $P2_1/c$, respectively. The bond length 1.147(2) Å of C(9)—N (1) in compound **4** is typical for a triple bond. Although compound **6** has a little bulky benzyl group, the bond angle of C (6)—C(7)—C(8) almost stays the same with only slight difference of 2° compared to reported DAP with alkyl chain group.[17]

NMR Spectra

The structure of ligand **9** was fully analyzed by ^1H and ^{13}C NMR along with 2-D ^1H–^1H COSY, ^1H–^{13}C HSQC, and ^1H–^{13}C HMBC, as illustrated in Figures 1–3.

^1H–^1H COSY Spectrum has established the correlations between equivalent protons and adjacent protons. In the Figure 1, two doublets 3.69–3.78 ppm and 3.56–3.65 ppm can be ascribed to equivalent proton pairs at C18. The active hydrogen atoms give rise to the resonance at 7.91–8.43 ppm. From the ^{13}C NMR spectroscopy we can see that the signals observed at 156.27 and 156.30 ppm can be attributed to the C23 and C22, which are the aromatic carbons attached to $O_{phenolate}$ atoms. The resonances due to aromatic carbons can be located in the 115.28–156.30 ppm range. The resonances recorded in high field at 49.95, 47.84, 43.48, and 40.05 ppm can be assigned to C15, C14, C18, and C16, respectively while signal at 63.90 ppm can be attributed to the quaternary carbon C17. ^1H—^{13}C HSQC spectrum (Figure 2) shows the respective correlation between H18, H18' with C18. Aromatic carbons are confirmed throughout the correlations between the carbon and its neighboring proton by using HMBC spectrum. Figure 3 has shown that the H5 (H6) is correlated with the carbons C20 and C7 (C8) with 2*J*, and correlated with carbon C9 with 3*J* long-range connectivity. HMBC spectrum also shows that H14 (H18) is correlated with C19 (C21) with 2*J* long-range conductivities, and the correlation between H14 with C1 and C23 (H18 with C10 and C22) with the 3*J* long range connectivities. The appearances of cross peaks show the correlations of C24 with respective H15 and H16 with 3*J* long-range connectivities.

The $V^{IV}O$ complex was characterized by ^1H NMR using DMSO-d_6 solvent. However, a resolvable ^1H NMR spectrum could not be exactly measured and display only broad signals owing to paramagnetism of tetravalent vanadium.

IR Spectra

IR spectra (Figures S2–S6) were taken to validate the structures and exhibited characteristic bands corresponding to various functional groups in the 400–4000 cm^{-1} region. The imines N—H stretching frequencies of the free ligand **9** and $V^{IV}O$ complex are expected in the 3100–3500 cm^{-1} region. N-H stretching frequencies are shifted to a lower wavenumber, indicating the ligation of imines nitrogen to the metal vanadium, which is supported by the literature.[21] The bands ranged at 2800–3000 cm^{-1} are associated with the

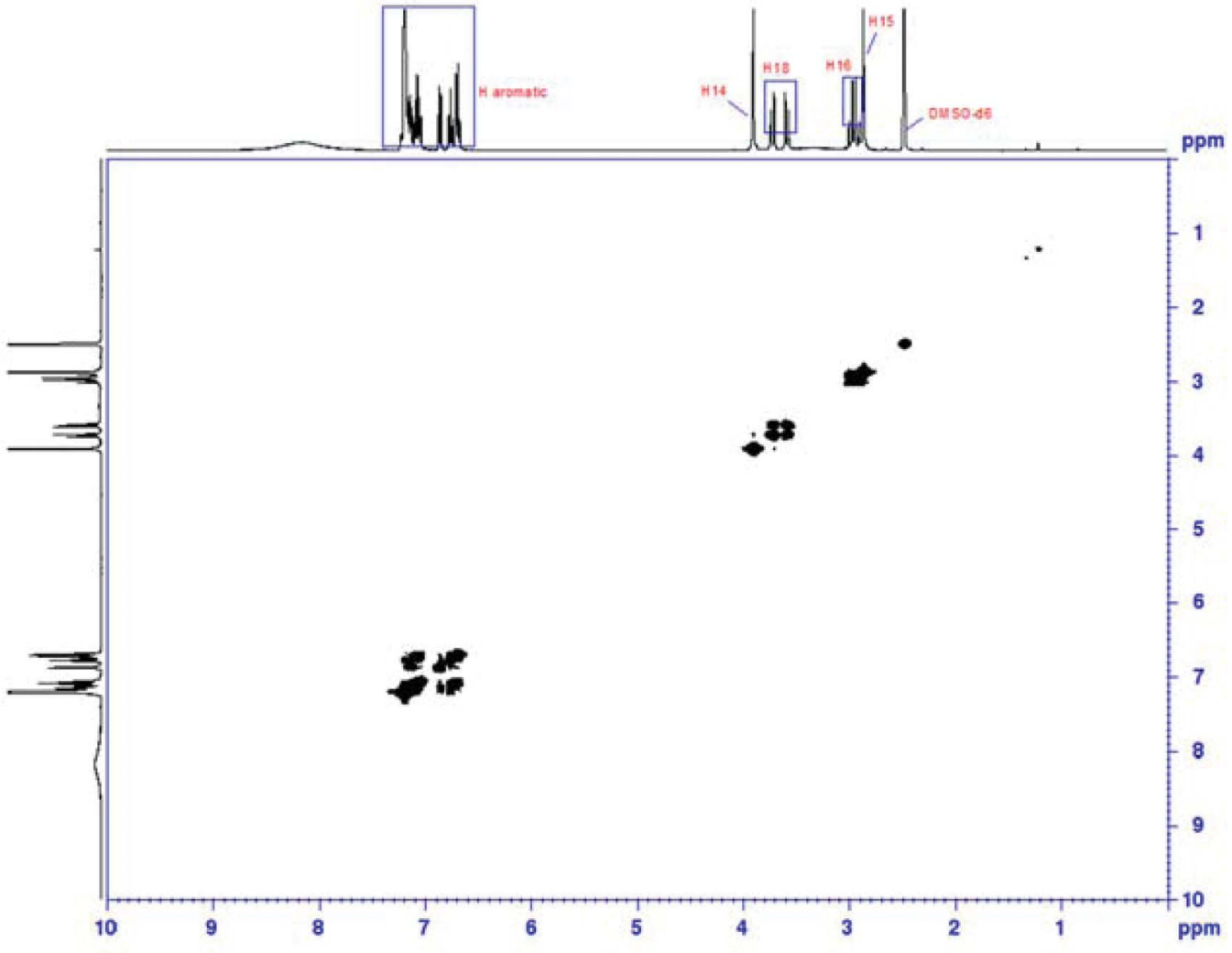

Fig. 1. ^{1}H–^{1}H connectivities in the COSY spectrum for ligand **9**.

asymmetric (γ_{as}) and symmetric (γ_{s}) stretching vibrations of aliphatic methylene (—CH_2—) and aromatic CH. Their frequencies and intensities nearly stay the same in changing from Schiff base ligand **9** to $V^{IV}O$ complex. The C=O stretching vibration ascribes at the band 1613 cm^{-1} in the Schiff base ligand and at the band 1639 cm^{-1} in the $V^{IV}O$ complex, respectively.[41] The carboxylate ion group -COO^{-} absorbs strongly at 1595 cm^{-1} in ligand and at 1596 cm^{-1} in complex as asymmetrical $C(=O)_2$ stretching, and more weakly at 1389 cm^{-1} in ligand and at 1391 cm^{-1} in complex as symmetrical $C(=O)_2$ stretching. C—N stretching absorption frequencies of the imines distribute in a wide range at 1020–1250 cm^{-1} and 1266–1342 cm^{-1} region.[42]

The strong and sharp V=O stretching band in the complex shows at 962 cm^{-1} similar to that of relevant references.[21,40,43] The assignments of vanadium-oxygen and vanadium-nitrogen are sometimes very difficult. As reported by Zamian,[43] V—O and V—N is tentatively assigned at 468 (w) cm^{-1} and 440 (m) cm^{-1} respectively, where the bands are observed as new absorption peaks and not exist in the spectrum of the free ligand **9**.

DFT Computations

Geometries of the neutral and deprotonated ligands

At the experimental condition, the possible complexation processes of Schiff base ligand (L) and $VOSO_4$ are as follows:

$$LH_3 + 3NaOH \rightarrow L^{3-} + 3Na^{+} + 3H_2O \quad (1)$$

$$VOSO_4 + 2NaOAc \rightarrow VO(OAc)_2 + Na_2SO_4 \quad (2)$$

$$L^{3-} + VO(OAc)_2 \rightarrow [VOL]^{-} + 2[OAc]^{-} \quad (3)$$

In order to predict preference on a specific configuration of the ligand **9**, R- and S- enantiomer, each of which covers four conformers differing in the relative position of two phenol hydroxyl groups, were considered to construct the neutral ligands in the calculations. These fully optimized stereoisomers of the neutral ligands are shown in Figure 4. R-conformers are more stable than S-type. Among the explored isomers of neutral ligand, L^{R}_d is the most stable with energy differences of more than 5 kcal mol^{-1} compared to other ligands. These optimized geometries were then used to prepare the

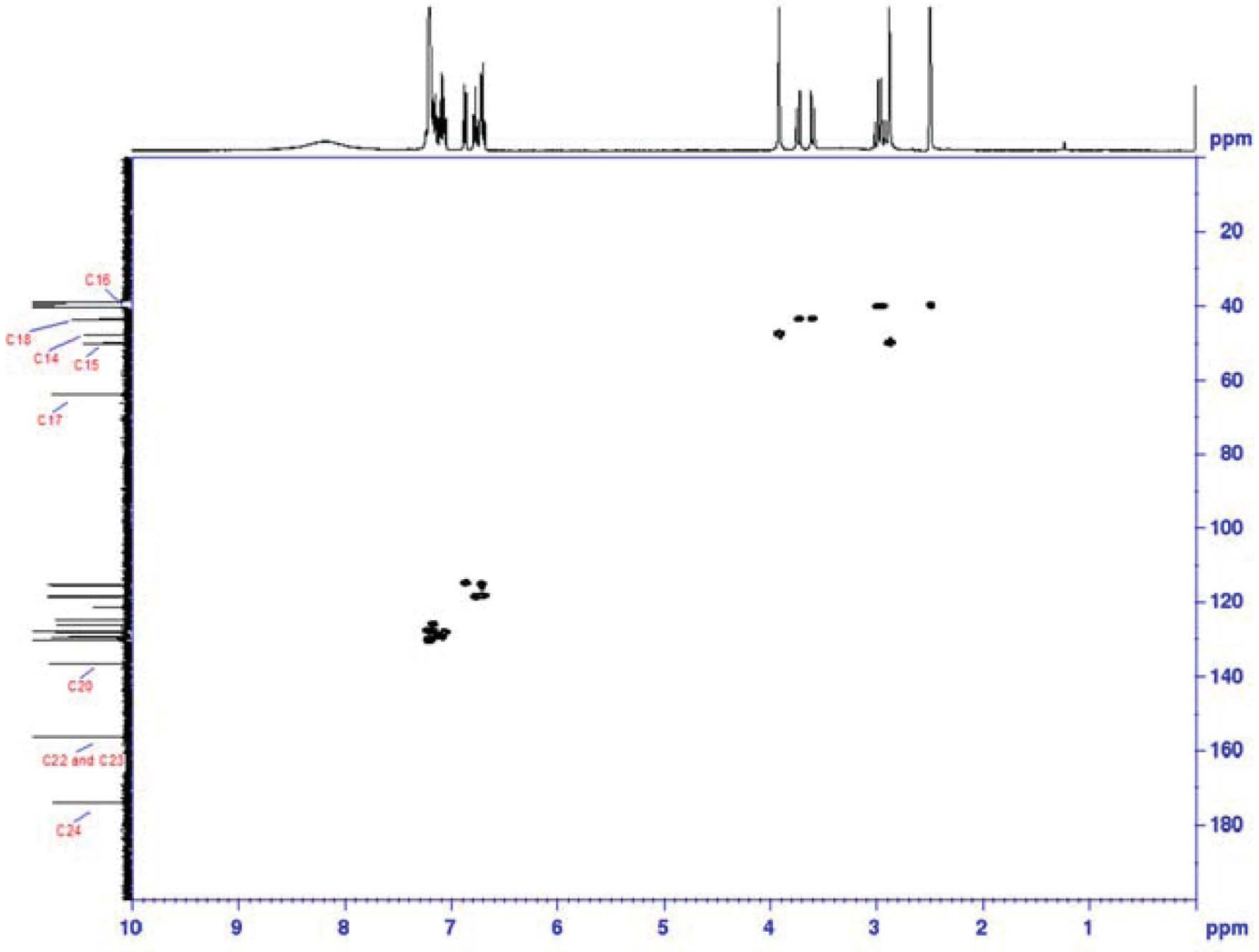

Fig. 2. One bond CH correlations in the HSQC spectrum for ligand **9**.

starting structures of corresponding deprotonated ligands, which were also fully optimized followed by vibrational frequency analysis. Results reveal that deprotonated L^S_d and L^R_b anions are thermodynamically minima. The electronic energy of L^S_d anion is slightly higher 1.05 kcal mol^{-1} than that of L^R_b anion, while others are more than 6.40 kcal mol^{-1} relative to L^R_b anion. Figure S7 illustrates the predicted IR spectra of deprotonated L^S_d and L^R_b anions. It seems that the predicted spectrum of L^R_b anion agrees well with that determined in experiment.

Structure of the $V^{IV}O$ Complex

We consider all possible coordination sites of deprotonated ligand anions to $V^{IV}O$ (i.e., in the initial guess V atom was coordinated to imine N or to O atoms of ligand **9**). In total there are 20 possible coordination situations for all deprotonated ligands. The computational results reveal four preferred complexes (R_$V^{IV}O$ Complex_a, R_$V^{IV}O$ Complex_b, S_$V^{IV}O$ Complex_c, and S_$V^{IV}O$ Complex_d), where V atom is coordinated to $O_{phenolate}$, $O_{carboxylate}$, or N_{imine}. Their structures and natural bond orbital diagram are illustrated in Figure 5. Mayer bond order analysis of four complexes and the relative electronic energies of complexes, Gibbs free energies of the complexing reactions, and deformation energies of ligands for four complexes are listed in Table 1.

Figure 5 discloses that R_$V^{IV}O$ Complex_a has the coordination sites of V atom with 2 × $O_{phenolate}$ and 2 × N_{imine} donors, forming a tetradentate complex. HOMO-11 and HOMO-13 of R_$V^{IV}O$ Complex_a show the interaction of V with O and N, respectively. The NBO analysis indicates that O27 coordinated with V has major contribution to orbital HOMO-11. The contribution consists of d-shells of V (22.9%) and p-shells of O27 (36.0%), O30 (18.6%), and N26 (8.5%). Orbital HOMO-13 mainly consists of d-shells of V (16.2%) and p-shells of N25 (7.2%) and N26 (7.4%). The composition of these orbitals indicates that V atom coordinated to $O_{phenolate}$ takes precedence over other sites in R_$V^{IV}O$ Complex_a, which is in accord with the Mayer bond order analysis shown in Table 1, where the bond orders of V with O27 and O30 are 0.86 and 0.83, respectively. These

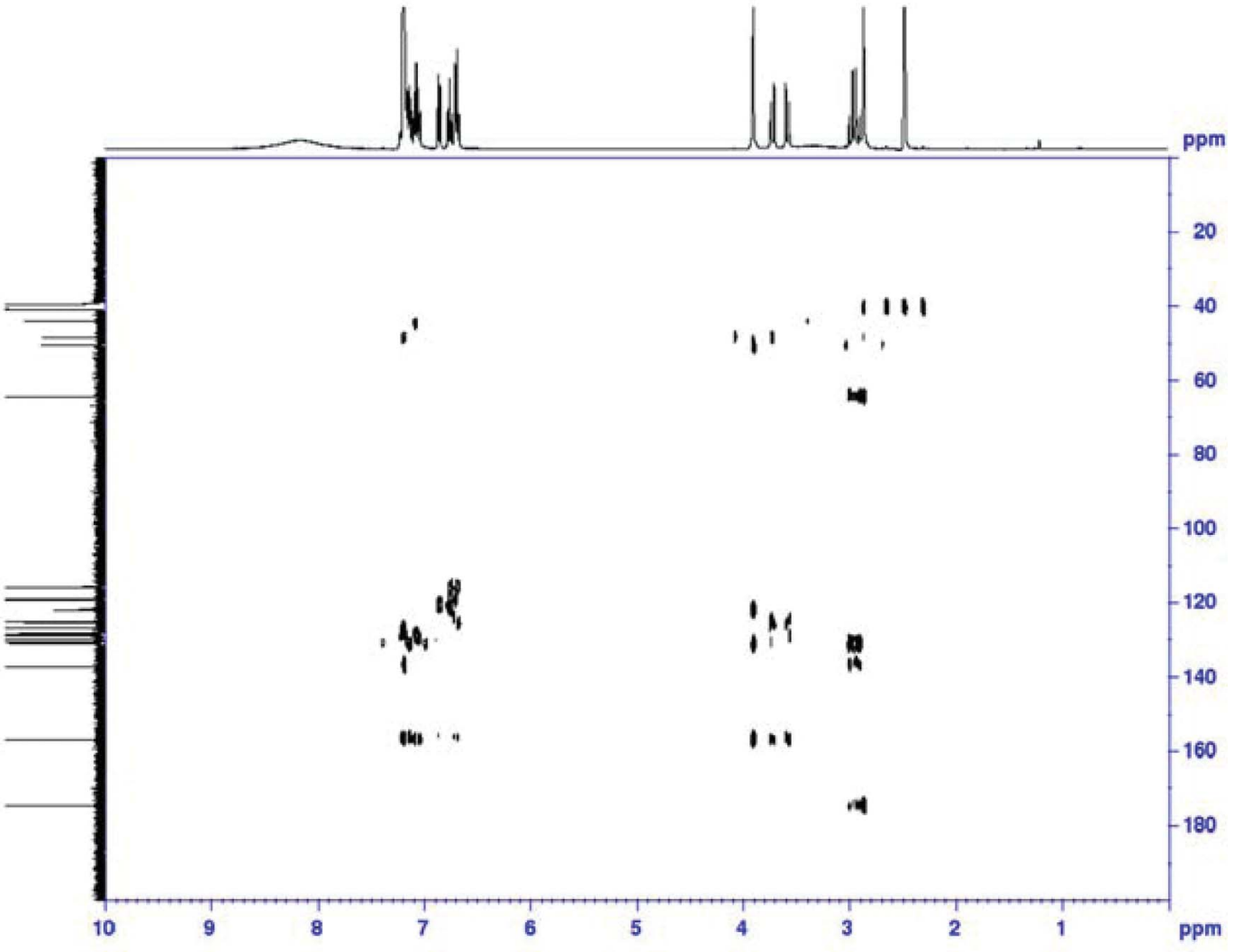

Fig. 3. Long range CH correlations in the HMBC spectrum for ligand **9**.

two bonds are stronger than that between V and N25 or N26 (0.46 and 0.52, respectively).

Similarly, it can be concluded that R_$V^{IV}O$ Complex_b forms tridentate complex with V−O30, V−O28, and V−N25 coordination bonds, in which V binds to $O_{carboxylate}$ instead of 2 × $O_{phenolate}$. S_$V^{IV}O$ Complex_c has three-coordination bonds of V−O30, V−O27, and V−N26, while S_$V^{IV}O$ Complex_d is tetra-coordinated ones.

From Mayer bond order analysis, it can be shown that V coordinated to O is of priority relative to N atom in four complexes. This can be explained according to Pearson's hard soft acid base (HSAB) principle,[44] which states that the hard and soft cations prefer to complex to hard and soft electron donors, respectively. The stability of complexes formed largely depends on the nature of the electron donor atoms present in the ligand. In term of HSAB theory, $[V^{IV}O]^{2+}$ is classified as hard acids, while the charged $O_{phenolate}$ and $O_{carboxylate}$ are harder bases than N_{imine}. Hence, V atom binds to O stronger than to N during complexation.

In order to further understand the stability of four complexes, the relative electronic energies of complexes, Gibbs free energies of complexing reactions, and deformation energies of ligands are calculated at B3LYP/6-31G* level. It can be shown from Table 1 that R_$V^{IV}O$ Complex_a is located as the most thermodynamically stable minimum among all complexes due to the lowest relative electronic energy. The Gibbs free energy of R_$V^{IV}O$ Complex_a is the lowest (i.e., –814.87 kcal mol^{-1}), which reveals that forming of R_$V^{IV}O$ Complex_a is relatively dominant. In addition, the deformation energies of ligands in R-type complexes are lower than those in S-type ones, in which the deformation energy is defined as the energy difference between the ligand in complex and free ligand ion. The larger deformation energy indicates the larger strain in complex. Obviously, from the relative electronic energy, reaction free energy and deformation energy of ligand in complex, it can be suggested that R_$V^{IV}O$ Complex_a is easy to form and identified as the lowest-lying stationary point.

Theoretical IR spectra of four complexes are shown in Figure S8. It can be found that the spectra of R-type complexes are much closer agreement with the experimental observations relative to S-type ones. Accordingly, R_$V^{IV}O$

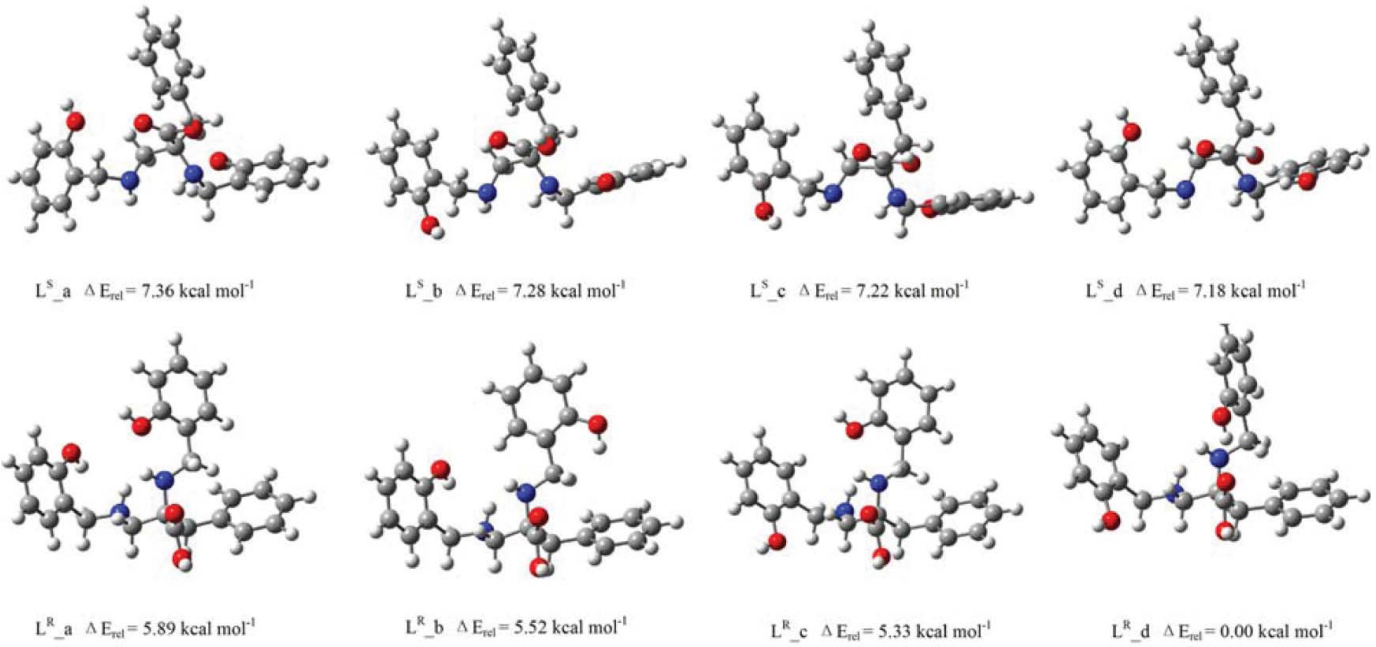

Fig. 4. The stereoisomers of the neutral ligand and their relative energies with zero-point energy correction at B3LYP/6-31G* level.

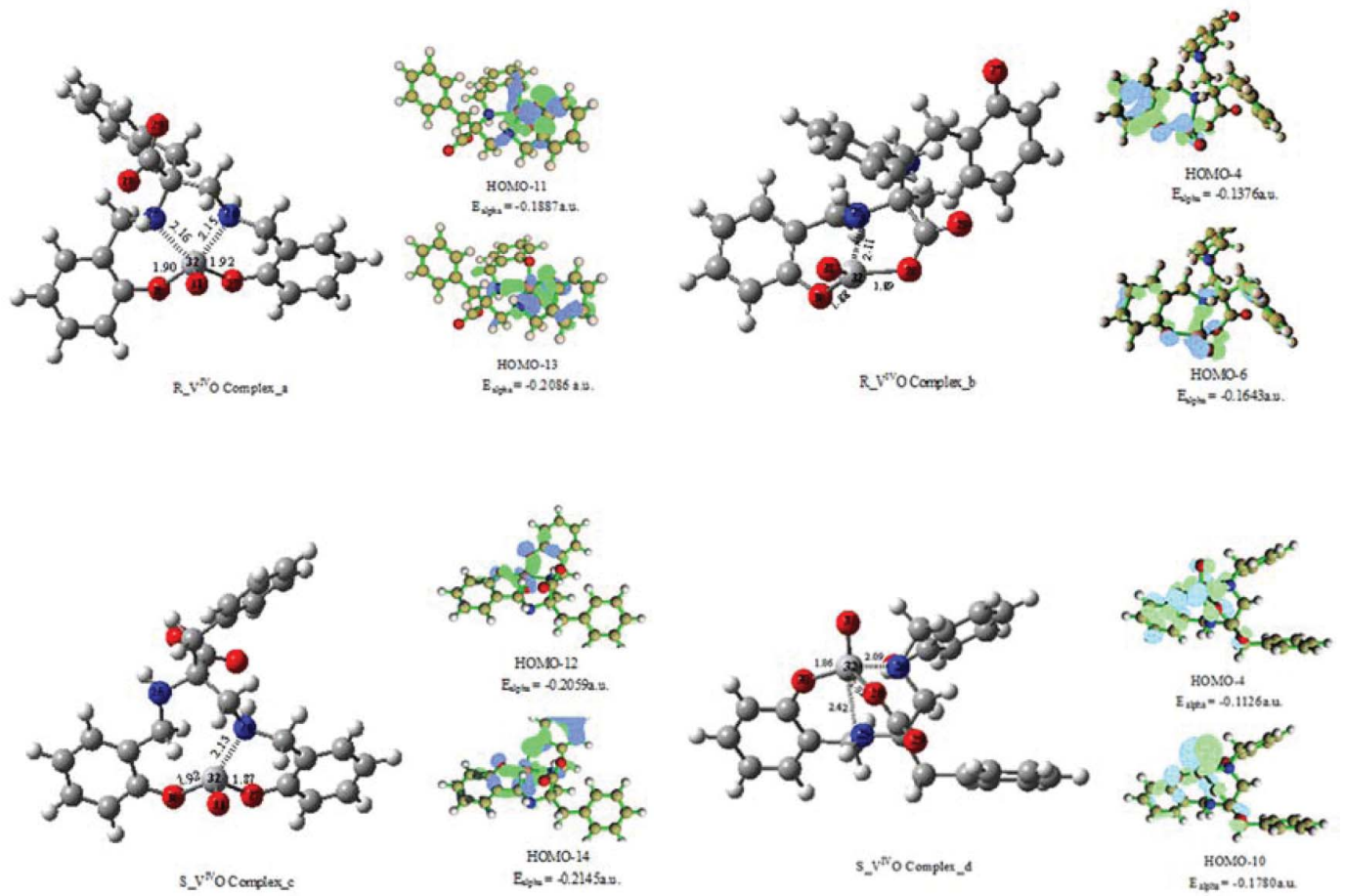

Fig. 5. The predicted structures of $V^{IV}O$ complex and natural bond orbital diagram at B3LYP/6-31G* level (V atom is labeled as No.32).

Complex_a is predicted as the most possible structure in the present study from the viewpoint of the thermochemistry.

ESI-MS Spectra

ESI-MS spectra of the ligand **9** and its $V^{IV}O$ complex are depicted in Figure 6. Overall, the suggested structural formulae are further confirmed by analysis data, and the results are in agreement with a metal/ligand ratio of 1:1 in the $V^{IV}O$ complex.

The molecular ion peak for **9** is observed at *m/z* 407.1944 corresponding to [M + H]. This species by the loss of $-CH_2-C_6H_4-O-$ section produces a fragment ion [M—C_7H_6O + H] at *m/z* 301.1537. The molecular ion peaks observed at 813.3821 and 1219.5643 corresponds to [2M + H] and [3M + H], respectively. A molecular ion peak of the $V^{IV}O$ complex shown at *m/z* 493.0867 is equivalent to the molecular weight of its parent ion. Removing a sodium ion from this molecular gives a fragment ion peak at *m/z* 471.1055 corresponding to the [M—Na + H] species. The molecular ion continuously undergoes demetallation to give a fragment ion peak at *m/z* 407.1902, which belongs to [M—Na-VO+4H] species equivalent to the ligand **9**. The molecular ion peaks are shown at 963.1832 and 1433.2801, corresponding to [2M-Na] and [3M-2Na], respectively.

In Vitro *Biological Evaluation*

Antibacterial activities were qualitatively screened by using Gram-positive bacteria, namely *S. aureus*, *L. acidophilus*, and *E. faecalis*, and a Gram-negative bacterium *E. coli*. Pure DMSO as a reference did not show any inhibition against the tested bacteria. Table 2 shows the comparative data by measuring the diameter of inhibition zone. Schiff base ligand **9** showed no antibacterial activity against all the four strains. A clear zone around each disk indicates that the growth of

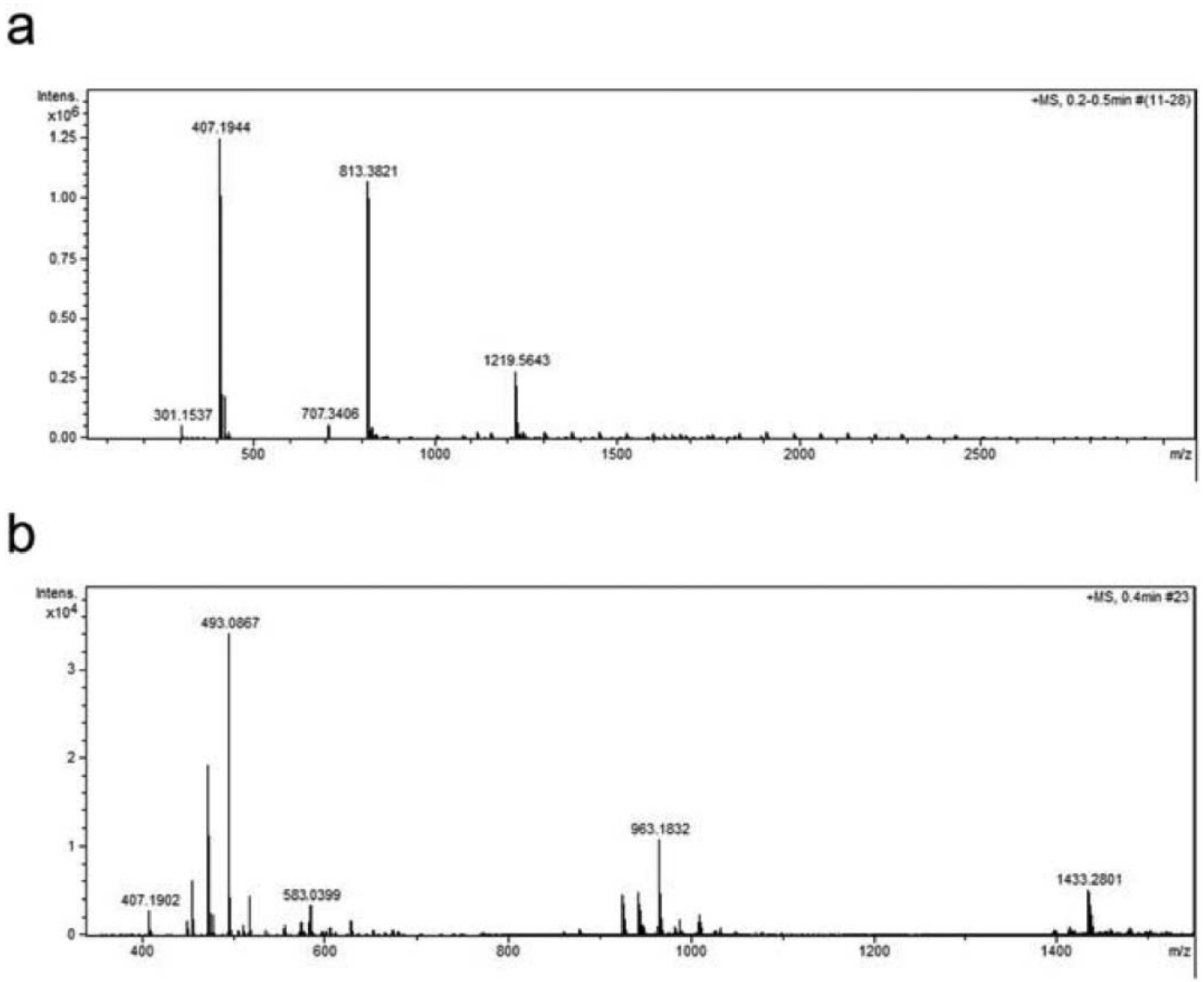

Fig. 6. ESI-mass spectra of ligand **9** (a) and $V^{IV}O$ complex (b) in the positive mode (the data shown are on the top traces).

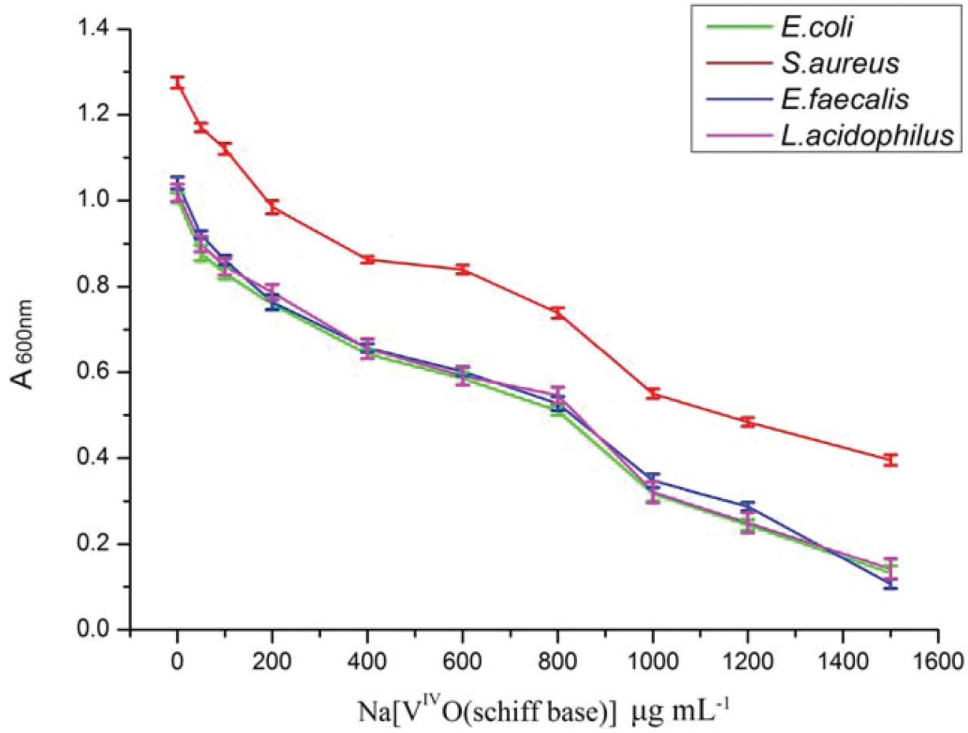

Fig. 7. Inhibition growth curves of $V^{IV}O$ complex against *S. aureus*, *L. acidophilus*, *E. faecalis*, and *E. coli*.

microbes is evidently inhibited in the presence of $V^{IV}O$ complex. The inhibitory ratios against above microbes are all above 50% compared with standard kanamycin as positive control. The inhibitory effect of $V^{IV}O$ complex on the bacterial growth was recorded spectrophotometrically after incubation. From the growth-inhibitory curves in Figure 7 we can see clearly that antibacterial activity is concentration dependent: with the increasing concentration ranging from 0 to 1500 μg mL^{-1}, the absorbance at 600 nm decreases. Hence, it demonstrates that $V^{IV}O$ complex can perform as an inhibitor on the bacterial growth.

Schiff base ligand **9** and $V^{IV}O$ complex were chosen to evaluate in the cytotoxicity assays due to the lower toxicity than that of vanadate.[45] CCK-8 assay was used to determine cellular survival rates at a particular time when exposed to cytotoxic complex. As shown in Figure 8, ligand **9** is not remarkable towards the tumor cells. The $V^{IV}O$ complex presents greater antitumor activity *in vitro* against both *A549* and *Hela* cell lines compared with free ligand as negative control. The inhibitory action is strengthened with the concentration increases. In above biological assays, both Schiff base ligand **9** and $V^{IV}O$ complex were distributed homogeneously

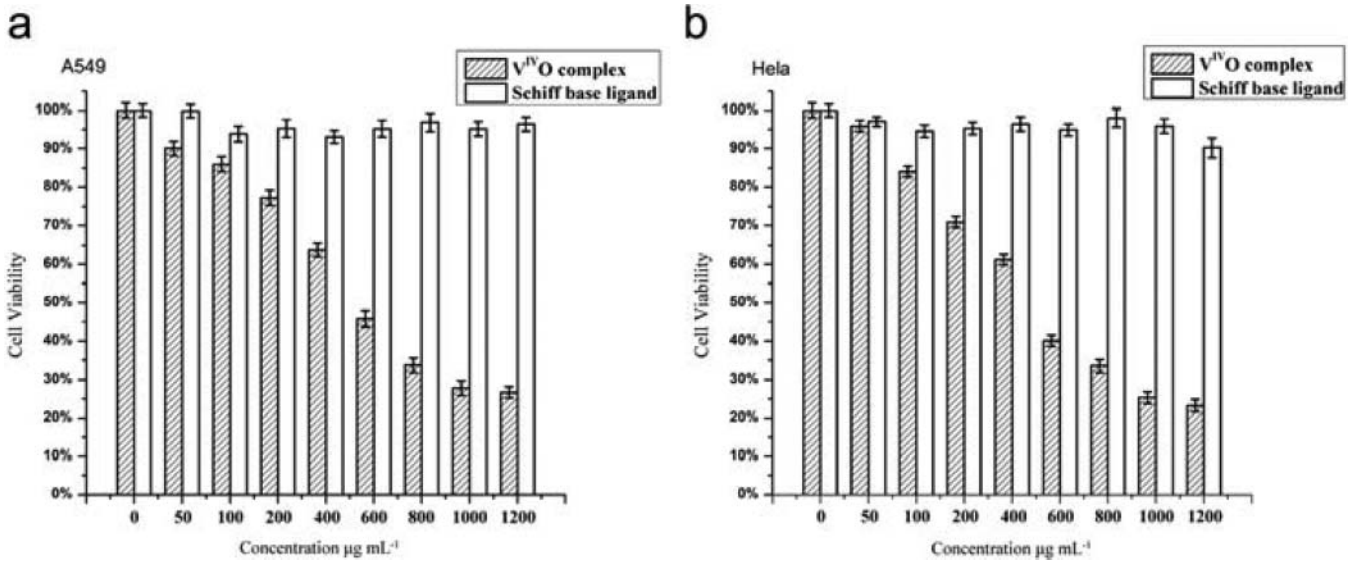

Fig. 8. Cell viability of Schiff base ligand **9** and $V^{IV}O$ complex on growth inhibition on *A549* (a) and *Hela* (b).

in the form of emulsion, and showed excellent stability in the culture medium without precipitation phenomenon. A brief summary drawn from the previous *in vitro* biological evaluation is that the $V^{IV}O$ complex has shown inhibitory activities toward either the bacteria or the tumor cells and exhibits the potential as antibacterial and antitumor pharmaceuticals.

Conclusions

We have described the synthesis of $V^{IV}O$ complex of reduced Schiff base derived from phenylalanine analogue containing DAP. The composition and chemical properties are characterized and analyzed. Theoretical study has been conducted and presents the most probable binding mode. *In vitro* biological evaluation, the $V^{IV}O$ complex shows enhanced activity as antibacterial agents against both Gram-negative and Gram-positive bacteria as well as antitumor activity against two tumor cell lines. DFT computations in this paper may provide theoretical base for the description and explanation of Schiff base complexes containing DAP. In addition, the present study displays a perspective of using this kind of metal complexes as antibacterial and antitumor pharmaceuticals in medical field. Further research of this high-denticity ligand to other metal analogues is in progress.

Funding

This research is supported by One Hundred Person Project of the Chinese Academy of Sciences (Grant No. 292011312D1117110). The Supercomputing Center of Chinese Academy of Sciences is gratefully acknowledged for providing the computational resources.

Supplementary Material

Experimental and theoretical predicted IR spectra, ORTEP presentations and crystal data for CCDC-936085 (**4**) and CCDC-936084 (**6**) are supported. Crystallographic data can be also acquired free of charge via http://www.ccdc.cam.ac.uk/conts/retrieving.html, or from the Cambridge Crystallographic Data Centre, 12 Union Road, Cambridge CB2 1EZ, UK; E-mail: deposit@ccdc.cam.ac.uk.

References

1. Yoon, T. P.; Jacobsen, E. N. *Science* **2003**, *299*, 1691.
2. Nakayama, Y.; Bando, H.; Sonobe, Y.; Fujita, T. *J. Mol. Catal. A: Chem.* **2004**, *213*, 141.
3. Vetter, A. H.; Berkessel, A. *Tetrahedron Lett.* **1998**, *39*, 1741.
4. Leung, W. H.; Chan, E. Y. Y.; Chow, E. K. F.; Williams, I. D.; Peng, S. M. *Dalton Trans.* **1996**, 1229.
5. Schaus, S. E.; Branalt, J.; Jacobsen, E. N. *J. Org. Chem.* **1998**, *63*, 403.
6. Shi, L.; Mao, W. J.; Yang, Y.; Zhu, H. L. *J. Coord. Chem.* **2009**, *62*, 3471.
7. Bolm, C.; Bienewald, F. *Angew. Chem., Int. Ed.* **1995**, *34*, 2640.
8. Bolm, C.; Bienewald, F. *Synlett* **1998**, 1327.
9. Verquin, G.; Fontaine, G.; Bria, M.; Zhilinskaya, E.; Abi-Aad, E.; Aboukais, A.; Baldeyrou, B.; Bailly, C.; Bernier, J. L. *J. Bio. Inorg. Chem.* **2004**, *9*, 345.
10. Colpas, G. J.; Hamstra, B. J.; Kampf, J. W.; Pecoraro, V. L. *Inorg. Chem.* **1994**, *33*, 4669.
11. Lewis, N. A.; Liu, F. G.; Seymour, L.; Magnusen, A.; Erves, T. R.; Arca, J. F.; Beckford, F. A.; Venkatraman, R.; Gonzalez-Sarrias, A.; Fronczek, F. R.; Vanderveer, D. G.; Seeram, N. P.; Liu, A. M.; Jarrett, W. L.; Holder, A. A. *Eur. J. Inorg. Chem.* **2012**, 664.
12. Cole, B. M.; Shimizu, K. D.; Krueger, C. A.; Harrity, J. P. A.; Snapper, M. L.; Hoveyda, A. H. *Angew. Chem., Int. Ed.* **1996**, *35*, 1668.
13. Corrigan, J. J.; Srinivasan, N. G. *Biochemistry* **1966**, *5*, 1185.
14. Meierhenrich, U. J.; Muñoz Caro, G. M.; Bredehoft, J. H.; Jessberger, E. K.; Thiemann, W. H.-P. *Proc. Natl. Acad. Sci. USA* **2004**, *101*, 9182.
15. Liu, Y.; Pak, J. K.; Schmutz, P.; Bauwens, M.; Mertens, J.; Knight, H.; Alberto, R. *J. Am. Chem. Soc.* **2006**, *128*, 15996.
16. Park, Y.; Kang, S.; Lee, Y. J.; Kim, T. S.; Jeong, B. S.; Park, H. G.; Jew, S. S. *Org. Lett.* **2009**, *11*, 3738.
17. Liu, Y.; Oliveira, B. L.; Correia, J. D. G.; Santos, I. C.; Santos, I.; Spingler, B.; Alberto, R. *Org. Biomol. Chem.* **2010**, *8*, 2829.
18. Schley, M.; Fritzsche, S.; Lönnecke, P.; Hey-Hawkins, E. *Dalton Trans.* **2010**, *39*, 4090.
19. Faneca, H.; Figueiredo, V. A.; Tomaz, I.; Goncalves, G.; Avecilla, F.; De Lima, M. C. P.; Geraldes, C. F. G. C.; Pessoa, J. C.; Castro, M. M. C. A. *J. Inorg. Biochem.* **2009**, *103*, 601.
20. Jancso, A.; Paksi, Z.; Mikkola, S.; Rockenbauer, A.; Gajda, T. *J. Inorg. Biochem.* **2005**, *99*, 1480.
21. Costa Pessoa, J.; Marcão, S.; Correia, I.; Goncalves, G.; Dörnyei, A.; Kiss, T.; Jakusch, T.; Tomaz, I.; Castro, M. M. C. A.; Geraldes, C. F. G. C.; Avecilla, F. *Eur. J. Inorg. Chem.* **2006**, *2006*, 3595.
22. Koch, W.; Hertwig, R.; Schleyer, P. V. R. *Encyclopedia of Computational Chemistry*; Wiley, Chichester, England, **1998**.
23. Yu, G.; Wang, S. Z.; Wang, K.; Hu, Y. F.; Hu, H. W. *Synthesis* **2004**, 1021.
24. Otwinowski, Z.; Minor, W. *Methods Enzymol.* **1997**, *276*, 307.
25. Sheldrick, G. M. *Acta Crystallogr.* **2008**, *A64*, 112.
26. Barnes, C. L. *J. Appl. Cryst.* **1997**, *30*, 568.
27. Frisch, M. J.; Trucks, G. W.; Schlegel, H. B.; Scuseria, G. E.; Robb, M. A.; Cheeseman, J. R.; Scalmani, G.; Barone, V.; Mennucci, B.; Petersson, G. A. *Gaussian 09 Program*; Gaussian, Inc., Wallingford, CT, **2009**.
28. Parr, R. G.; Yang, W. *Density Functional Theory of Atoms and Molecules*; Oxford University Press, New York, **1989**.
29. Becke, A. D. *J. Chem. Phys.* **1993**, *98*, 5648.
30. Stephens, P. J.; Devlin, F. J.; Chabalowski, C. F.; Frisch, M. J. *J. Phys. Chem.* **1994**, *98*, 11623.
31. Becke, A. D. *Phys. Rev. A* **1988**, *38*, 3098.
32. Lee, C. T.; Yang, W. T.; Parr, R. G. *Phys. Rev. B* **1988**, *37*, 785.
33. Dolg, M.; Wedig, U.; Stoll, H.; Preuss, H. *J. Chem. Phys.* **1987**, *86*, 866.
34. Martin, J. M. L.; Sundermann, A. *J. Chem. Phys.* **2001**, *114*, 3408.
35. Hariharan, P. C.; Pople, J. A. *Theor. Chim. Acta* **1973**, *28*, 213.
36. Foresman, J. B.; Frisch, A. *Exploring Chemistry with Electronic Structure Methods*, 2nd edn.; Gaussian, Inc., Pittsburgh, PA, **1996**.
37. Sukanya, D.; Evans, M. R.; Zeller, M.; Natarajan, K. *Polyhedron* **2007**, *26*, 4314.
38. Shrivastava, H. Y.; Devaraj, S. N.; Nair, B. U. *J. Inorg. Biochem.* **2004**, *98*, 387.

39. Musa, M. A.; Khan, M. O.; Aspedon, A.; Cooperwood, J. S. *Lett. Drug Des. Discov.* **2010**, *7*, 165.
40. Selbin, J. *Coord. Chem. Rev.* **1966**, *1*, 293.
41. Simons, W. W. *The Sadtler Handbook of Infrared Spectra*; Sadtler Research Laboratories, Philadelphia, PA, **1978.**
42. Silverstein, R. M.; Webster, F. X.; Kiemle, D. J. *Spectrometric Identification of Organic Compounds*, 7th edn.; Wiley, New York, 2005.
43. Zamian, J. R.; Dockal, E. R. *Transition Met. Chem.* **1996**, *21*, 370.
44. Pearson, R. G. *J. Am. Chem. Soc.* **1963**, *85*, 3533.
45. Lu, J. Z.; Guo, J. W.; Sang, W.; Guo, H. W. *Transition Met. Chem.* **2013**, *38*, 481.